Trans Indian Inst Met (2020) 73(11):2875–2888
https://doi.org/10.1007/s12666-020-02088-3

ORIGINAL ARTICLE

Investigation on the Kinetics and Mechanism of Aluminothermic Reduction of Molybdenum Trioxide: Non-isothermal Kinetics

K. Sheybani[1] · M. H. Paydar[1] · M. H. Shariat[1]

Received: 18 March 2020 / Accepted: 6 September 2020 / Published online: 25 September 2020
© The Indian Institute of Metals - IIM 2020

Abstract In this work, effect of milling process and CaO addition on the reaction mechanism and kinetics of aluminothermic reduction of molybdenum trioxide were studied by simultaneous thermal analysis, differential scanning calorimetry, X-ray diffraction analysis and Coats–Redfern method, respectively. For this purpose, molybdenum trioxide was reduced by Al powder under two different conditions of mechanical activation by milling process and as received form mixed by stoichiometric amount of CaO that was required for creation of $CaMoO_4$ intermediate phase. In the case of using milled molybdenum trioxide, 20 wt% of aluminum oxide was used as heat absorber. The results showed that by using mechanically activated MoO_3, the reduction reactions proceeded through the formation of intermediate phases of $Al_2(MoO_4)_3$ and MoO_2. In the presence of CaO, the intermediate phase was changed to $CaMoO_4$. In both cases, the reaction temperatures and their activation energies decreased. The kinetic model for the aluminothermic reduction of un-milled and milled molybdenum trioxide was determined as chemical control, where by addition of CaO, mechanism of the reduction reaction was changed to diffusion control.

Keywords Kinetic · Mechanism · Molybdenum trioxide · Aluminothermic reduction · Mechanical activation · Activation energy · Non-isothermal

✉ M. H. Paydar
paaydar@shirazu.ac.ir

[1] Department of Materials Science and Engineering, School of Engineering, Shiraz University, Shiraz, Iran

1 Introduction

Molybdenite (MoS_2) is the major source for production of molybdenum and its alloys [1]. Recently, many researchers suggested that combustion-based technology known as combustion synthesis (or self-propagation high-temperature synthesis) can be used for producing Mo powder [2–4]. They proposed that, metallothermic reduction of MoO_3 by Zn, Mg and Al, and carbothermic reduction of MoO_3 is a good method that can solve the problems of hydrogen reduction of MoO_3, which is carried out at different temperature steps and need a close system due to solid–gas reaction [5–7]. The conventional method for producing molybdenum and its alloys is based on roasting of molybdenite, followed by the purification of the resultant oxide (MoO_3) and finally reduction of the purified molybdenum oxide by high purity H_2 gas [2]. Recently, metallothermic reduction process has been suggested by few researchers for producing metallic molybdenum, in which Zn and Mg have been introduced as reducing agents [8–10]. The studies showed that metallothermic reduction of MoO_3 can be carried out successfully, and separation of molybdenum metal from zinc or magnesium oxides can be carried out by HCl leaching [11–13]. Recently, Sheybani et al. [14] showed that molybdenum trioxide can also be reduced to metallic Mo by using Al powder as reducing agent. They also studied the effect of mechanical activation on the aluminotherimc reduction of MoO_3 and showed that the reduction process could be initiated after 5 h, during milling process and mechanical activation increases the efficiency of the reduction reaction [14]. Furthermore, they calculated change in the adiabatic temperature of the reduction reaction as a function of the amount of used Al_2O_3 and showed that it can reduce adiabatic

temperature of the alumiothermic reduction of MoO_3 oxide and prevent its explosive mode. However, in that study, the mechanism and kinetics of aluminothermic reduction of molybdenum trioxide have not been investigated.

In the case of metallothermic reduction of MoO_3, one of the major problems is the sublimation of MoO_3 due to its high vapor pressure. In the present work, two different methods including mechanical activation and addition of CaO were suggested for reducing sublimation of MoO_3. Ataie et al. investigated the feasibility of producing nano-crystalline molybdenum by mechano-chemical reaction in MoO_3-C system. They showed that metallic molybdenum powder with a mean crystallite size of 45 nm can be produced through carbothermic reduction of highly mechanically activated MoO_3 [15]. In another studies, reaction pathway in the $MoO_3 + Mg + C$ mixtures was studied by Manukyan [8]. They studied reduction mechanism of mechanically activated MoO_3 by magnesium and carbon, as reducing agent. The effect of mechano-chemical process on the molybdenite's roasting kinetics was studied by Kahrizsangi et al. [16]. They showed that after 36h of mechanical activation by milling process, the ignition temperature of reaction decreases from 470 to 180 °C. By studying reduction reaction kinetics, they proved that mechanical activation can increase reducing rate of MoO_3 by changing its mechanism [16].

Thermodynamic studies of MoO_3–C system with the help of TGA analysis showed that, there is a mass loss in the temperature range of 700–900 °C due to sublimation of MoO_3, whereas by addition of CaO, in the CaO–C–MoO_3 system, less mass loss is recorded during the reduction process due to the reaction of CaO with MoO_3 [17]. In fact, CaO combines with MoO_3 almost at low temperature, according to the following reaction, and prevent its sublimation:

$$MoO_3 + CaO = CaMoO_4 \quad (1)$$

Based on the literatures, it can be realized that mechanical activation and also addition of CaO can change the mechanism and kinetics of aluminothermic reduction of molybdenum trioxide. However, there is no report about reaction pathway and the effect of mechanical activation together with CaO addition on the reaction mechanism, rate of aluminothermic reduction and sublimation of molybdenum trioxide. Therefore, purpose of the present study is to gain more quantitative insights into the mechanisms and kinetics of aluminothermic reduction of MoO_3. Furthermore, the effect of mechanical activation and CaO addition on the kinetics, mechanism of the reduction reaction and on the restraining evaporation of MoO_3 has been investigated.

2 Experimental

2.1 Materials

Molybdenum trioxide, metallic aluminum, aluminum oxide and calcium oxide powders were used as raw materials. Molybdenum trioxide powder with 98% purity and − 325 mesh size was prepared from Sarcheshmeh-Kerman-Iran industry. Calcium oxide (99% purity and 100 μm) and aluminum oxide (99% purity) powders supplied by Merck Company and aluminum powder (99% purity) from powder metallurgy of Khorasan-Iran Company in the size range of less than 150 μm were used as reducing agent. Argon gas with 99.999% purity was used as the protective gas during the heating of samples to prevent aluminum reaction with oxygen at elevated temperatures.

2.2 Apparatus and Procedure

In this research, two different mixtures were prepared. In the first mixture, molybdenum trioxide was mechanically activated by milling process at different times and then was mixed with the stoichiometric amount of aluminum, according to reaction (2). Aluminum oxide, equal to 20 wt. % of the mixture, was also added as heat absorber.

$$MoO_3(s) + 2Al(s) = Mo(l) + Al_2O_3(l) \quad (2)$$

For mechanical activation of the prepared mixture, a planetary ball mill under argon atmosphere was used with a 15:1 ball to powder weight ratio. Stainless steel vial and balls with 20 mm diameter were used as the milling container and media, respectively. The milling process was carried out for 5, 10 and 24 h. In the second mixture, the as-received MoO_3 was mixed with Al and CaO with stoichiometric ratio. The amount of CaO was selected according to reaction (1).

The reduction reactions were studied using a simultaneous thermal analysis (STA) system. The reaction tube of the used STA system was heated up in a non-isothermal mode from room temperature to 1100 °C with a linear heating rate of 10 °C min^{-1} under pure argon gas flow. The initial weight of the used samples was about 30 mg. All the solid products were analyzed using X-ray diffraction by Philips X-ray diffractometer using Cu Kα radiation over a 2θ range of 10–90° and 2 s count time for every 0.05° step. Morphology, composition and microstructures of the heated samples were studied using a scanning electron microscope (SEM), equipped with energy-dispersive spectroscopy (EDS) system. The kinetics of reduction reaction was analyzed by using Coats–Redfern method, and the HSC software was used for thermodynamic calculations.

3 Results and Discussion

3.1 Thermal Analysis of Mechanically Activated MoO_3–Al–Al_2O_3

To prevent the explosion that may happen by the reaction of MoO_3 with Al and to reduce the adiabatic temperature of the reaction, aluminum oxide equivalent to 20 wt% of the reactants was used as heat absorber in the initial mixture of the samples before carrying out STA tests [14]. Figure 1 shows the differential scanning calorimeter (DSC) analysis of the as received and mechanically activated MoO_3 in different times, after mixing with the appropriate amount of Al and Al_2O_3 powders.

As evidenced in Fig. 1, the aluminothermic reduction of MoO_3 can be characterized by three peaks in DSC curves and as it can be seen that mechanical activation does not only eliminates the peaks but causes a change in their locations. According to Fig. 1, the second and third peaks occur at 850 and 1100 °C, respectively, where they are shifted to the lower temperatures due to use of mechanically activated MoO_3. This is a clear indication of the effect of mechanical activation on decreasing the reduction temperature of MoO_3. The first endothermic peak at around 660 °C is due to the melting of Al powder. As the Al powder is not mechanically activated, no shift of this peak has been recorded for all the three samples. The second and third peaks are due to the exothermic reactions. This means that aluminothermic reduction of molybdenum trioxide has advanced through the two steps [11, 13, 17]. In order to study mechanism of the reaction, the reduction products formed at these temperatures were analyzed by using XRD.

3.2 Investigation on the Mechanism of Aluminothermic Reduction of MoO_3 by Thermal Analysis

To study the mechanism of reaction and finding a reason for creation of the second peak in Fig. 1, the un-milled and 24-h milled samples were heated to 850 °C (ending temperature of second peak and before the starting of the third peak) under the same condition used in STA analysis. After completing the heating period, the products were air cooled and analyzed with XRD. Figure 2 shows the XRD patterns of un-milled $MoO_3 + Al + Al_2O_3$ and 24-h milled $MoO_3 + Al + Al_2O_3$ mixtures after heating to 850 °C.

According to Fig. 2, at 850 °C, strong peaks of intermediate phases of $Al_2(MoO_4)_3$ and MoO_2 have been identified. These findings indicate that aluminothermic reduction of molybdenum trioxide advances through the formation of intermediate phases of $Al_2(MoO_4)_3$ and MoO_2. As evidenced in Fig. 2, in the non-activated sample, the $Al_2(MoO_4)_3$ is more pronounced than for the 24-h milled sample. However, for both the mixtures including un-milled and milled samples heated up to 850 °C, the aluminum peaks could still be detected clearly. It means that, the remaining active Al is probably enough to reduce the created intermediate phases, in the final stage of the reduction process. The formation of MoO_2 indicates that reduction of MoO_3 by Al, proposed by reaction (2), is divided into two steps. In the first step, MoO_3 reduces to molybdenum dioxide (MoO_2) and finally MoO_2 is reduced by the remaining Al to Mo, according to reactions (3) and (4).

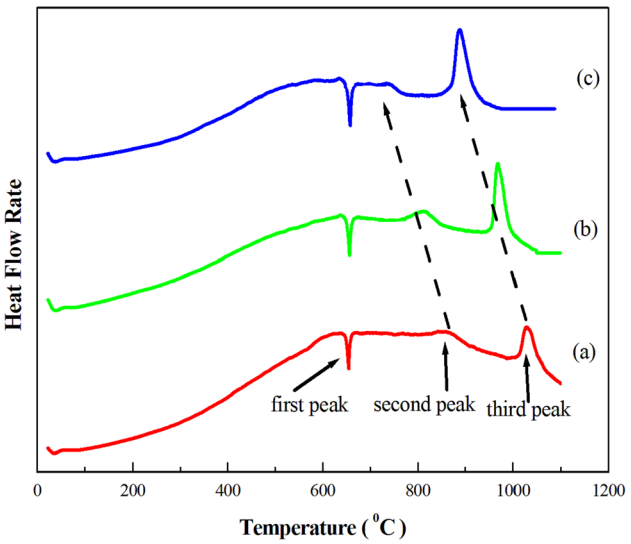

Fig. 1 DSC analysis of **a** un-milled $MoO_3 + Al + Al_2O_3$, **b** 5 h and **c** 24 h milled MoO_3 mixed with appropriate amount of Al and Al_2O_3

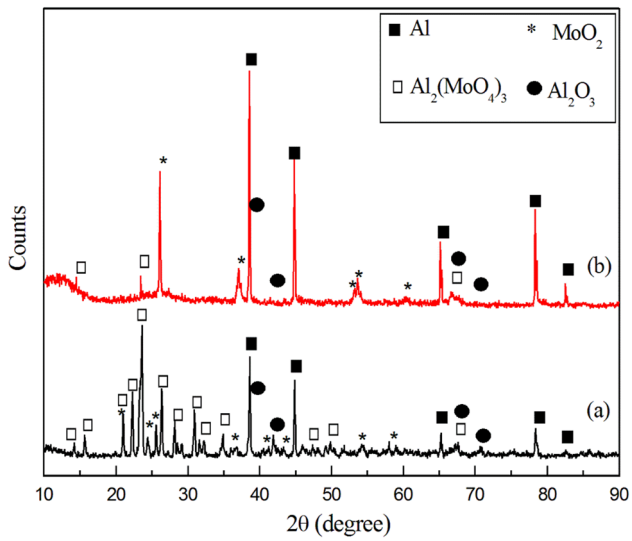

Fig. 2 XRD patterns of **a** un-milled $MoO_3 + Al + Al_2O_3$, **b** 24-h milled $MoO_3 + Al + Al_2O_3$, after heating up to 850 °C

$$3MoO_3 + 2Al = 3MoO_2 + Al_2O_3 \quad (3)$$

$$1.5MoO_2 + 2Al = 1.5Mo + Al_2O_3 \quad (4)$$

As it can be seen in XRD patterns presented in Fig. 2, no indication of unreacted MoO_3 phase in the intermediate products can be identified. This is an indication for completion of reaction (3). However, MoO_3 can also react with aluminum to form aluminum molybdate and molybdenum dioxide, according to reaction (5), to produce other intermediate phases [18].

$$6MoO_3 + 2Al = Al_2(MoO_4)_3 + 3MoO_2 \quad (5)$$

Reduction of $Al_2(MoO_4)_3$ can be carried out in two different routes. In the first path, according to reaction (6), $Al_2(MoO_4)_3$ dissociates to molybdenum dioxide and aluminum oxide; then molybdenum dioxide can be reduced to molybdenum according to the reaction (4). In the second path, $Al_2(MoO_4)_3$ reduces to molybdenum metal according to reaction (7) [18].

$$Al_2(MoO_4)_3 = 3MoO_2 + Al_2O_3 + 1.5O_2(g) \quad (6)$$

$$Al_2(MoO_4)_3 + 6Al = 3Mo + 4Al_2O_3 \quad (7)$$

Based on the XRD patterns presented in Fig. 2, it can be concluded that two intermediate phases of MoO_2 and $Al_2(MoO_4)_3$ can be produced. It means that the reactions (3) and (5) happen corresponding to the second peak and the reactions (4) and (7) correspond to the reduction of the intermediate phases to the final products, resulting in the third peak in Fig. 1.

Based on the thermodynamic parameters presented in Table 1, it can be understood that all the intermediate and final reactions are thermodynamically feasible at the reaction temperatures due to the high negative value of their $\Delta G°$.

According to Fig. 1, mechanical activation of MoO_3 decreases the reaction temperature at which intermediate phases are created. But for the non-activated MoO_3, MoO_2 and $Al_2(MoO_4)_3$ are formed according to reaction (5), due to need for applying higher temperature. The formation of molybdates (calcium, aluminum etc.) take place at higher temperatures [15, 17].

Figure 3 shows the SEM and EDS images of un-milled and 24-h milled $MoO_3 + Al + Al_2O_3$ mixtures after heating up to 850 °C. At least four different points of samples in any EDS analysis were analyzed. The results of all spots in samples show almost similar EDS analysis and one of them has been shown in this paper. The spot locations for EDS analysis are shown in the SEM images by red flashes.

According to Fig. 3, the SEM micrographs for the heat treated mixtures including un-milled (Fig. 3a) and milled (Fig. 3b) MoO_3 are completely different. For the sample including un-milled MoO_3, the particles of aluminum molybdate with regular cubic shape can be clearly recognized, while for the sample including 24-h milled MoO_3, MoO_2 particles with irregular shapes can be detected. EDS analysis (Fig. 3c) shows the elemental composition of Mo, Al and O that is an evidence for producing of MoO_2 with the remaining amount of Al that would be necessary for final reduction of MoO_2 according to reaction (4). To study the third peak in Fig. 1, the mixtures were heated to 1100 °C (ending temperature of third peak) and then air cooled and analyzed by X-ray method. Figure 4 shows the XRD patterns of the $MoO_3 + Al + Al_2O_3$ mixtures including un-milled and 24-h milled after heating up to 1100 °C.

As it can be seen in Fig. 4, the reduction of intermediate phases of $Al_2(MoO_4)_3$ and MoO_2 are carried out by aluminum powder completely so that metallic molybdenum and aluminum oxide are produced as final products after heating the samples up to 1100 °C. Based on the presented XRD patterns in Fig. 4, it is noticed that for the milled sample, no intermediate phases are detected, although for the sample including un-milled MoO_3, the final stage of the reduction reaction is not completed and MoO_2 intermediate phase can be detected in final products. Therefore, it can be concluded that mechanical activation increases the rate of reduction reaction so that no intermediate phases remain unreacted in the final products. Figure 5 shows the SEM micrographs of the $MoO_3 + Al + Al_2O_3$ mixtures including un-milled and 24-h milled MoO_3 after heating up to 1100 °C.

As it can be seen in Fig. 5, the final products of aluminothermic reduction of molybdenum trioxide in both activated and non-activated forms are metallic molybdenum and aluminum oxide. But, in the case of using activated MoO_3, according to Fig. 5b, particle size of the products is clearly smaller. Thus, completing the final stage of the reduction reaction in the activated MoO_3 is due to increasing the specific surface area by mechanical activation [14, 16].

3.3 Effect of CaO Addition on Aluminothermic Reduction of Molybdenum Trioxide

3.3.1 DSC Analysis of MoO_3–Al–CaO Mixture

To study the effect of CaO addition on the mechanism of aluminothermic reduction of molybdenum trioxide, as received MoO_3 was mixed with Al and CaO with stoichiometric ratio. In the MoO_3–Al mixture, Al_2O_3 has been used to reduce the adiabatic temperature and explosive mode of reaction [14], but in the aluminothermic reduction of MoO_3 in the presence of additional lime, Al_2O_3 is not necessary due to effect of lime on the reaction. The

Table 1 Thermodynamic assessments for intermediate and final reactions in the aluminothermic reduction of molybdenum trioxide without and with presence of CaO [18]

Reaction	T (°C)	$\Delta H°$ (kJ)	$\Delta G°$ (kJ)	log $K(T)$
$3MoO_3 + 2Al = 3MoO_2 + Al_2O_3$	600	− 1214.158	− 1119.58	66.983
	800	− 1239.07	− 1094.34	53.271
	1000	− 1397.21	− 1039.33	42.64
$1.5MoO_2 + 2Al = 1.5Mo + Al_2O_3$	800	− 825.425	− 744.19	36.226
	900	− 827.31	− 736.54	32.79
	1000	− 829.32	− 728.72	29.9
$6MoO_3 + 2Al = Al_2(MoO_4)_3 + 3MoO_2$	600	− 1330.9	− 891.33	53.32
	800	− 1444.66	− 777.68	37.85
	1000	− 1850.57	− 589	24.18
$Al_2(MoO_4)_3 + 6Al = 3Mo + 4Al_2O_3$	800	− 2684.34	− 2899.39	141.13
	900	− 2643.81	− 2921.35	130.08
	1000	− 2602.49	− 2946.61	120.9
$MoO_3 + CaO = CaMoO_4$	400	− 163.018	− 167.077	57.46
	600	− 163.101	− 168.27	43.39
	800	− 163.295	− 169.437	34.25
	1000	− 215.016	− 161.324	27.82
$CaMoO_4 + 2\ Al = Mo + CaO.Al_2O_3$	400	− 786.23	− 740.546	57.46
	600	− 798.04	− 725.34	43.39
	800	− 834.6	− 703.79	34.25
	1000	− 849.95	− 678.08	27.82

prepared MoO_3–Al–CaO mixture was used for DSC analysis. Figure 6 shows the result for DSC analysis of the MoO_3–Al–CaO mixture together with what obtained for the MoO_3–Al–Al_2O_3 mixture that has been previously presented in Fig. 1a.

Figure 6 shows that, the aluminothermic reduction of MoO_3 in the presence of lime (CaO) can be characterized by three peaks in DSC curves similar to what recorded for the $MoO_3 + Al + Al_2O_3$ mixture. But, there are significant differences between these two curves. According to Fig. 6, by addition of CaO, the second and third peaks occur at lower temperatures. In other words, addition of CaO leads to decreasing the reduction temperatures similar to what happened by using mechanically activated MoO_3. The other difference is that, the second peak in the $MoO_3 + Al + CaO$ analysis is endothermic, whereas in the $MoO_3 + Al + Al_2O_3$ mixture it is exothermic, and also the third peak for the $MoO_3 + Al + Al_2O_3$ mixture is very sharp and narrow, whereas in the $MoO_3 + Al + CaO$ mixture it is wide. This is due to the difference in model of the reaction in the presence of CaO. In fact, for the $MoO_3 + Al + Al_2O_3$ mixture, the model that accurately can be fitted to reaction is chemical control, whereas for the $MoO_3 + Al + CaO$ mixture the mechanism of reaction is diffusion control that has usually smaller rates compared to chemical control [19, 20]. More explanation about the used models including the required calculations has been presented and discussed in the following sections.

3.3.2 *Investigation on the Mechanism of Aluminothermic Reduction of MoO_3 in the Presence of Lime*

To study the mechanism of reaction in $MoO_3 + Al + CaO$ mixture and to find rational reasons for the second and third peaks, treatments similar to what was carried out earlier for the $MoO_3 + Al + Al_2O_3$ mixture was followed. In this treatment, $MoO_3 + Al + CaO$ mixture was heated to 850 °C (ending temperature of second peak and beginning of the third peak) and also up to 1100 °C (ending temperature of the third peak), under similar conditions as used in DSC analysis, including heating rate, holding time and use of the protective atmosphere. Figure 7 shows the XRD patterns of $MoO_3 + Al + CaO$ mixture after heating up to 850 and 1100 °C.

According to Fig. 7a, it can be concluded that the second peak in Fig. 6 is due to the formation of $CaMoO_4$ intermediate phase. Thus, with addition of CaO to the system of aluminothermic reduction of MoO_3, the intermediate phases of $Al_2(MoO_4)_3$ and MoO_2 are not formed and $CaMoO_4$ is formed instead. The formation of this phase was also recorded by other researchers who studied the carbothermic reduction of molybdenum trioxide in the presence of lime [17].

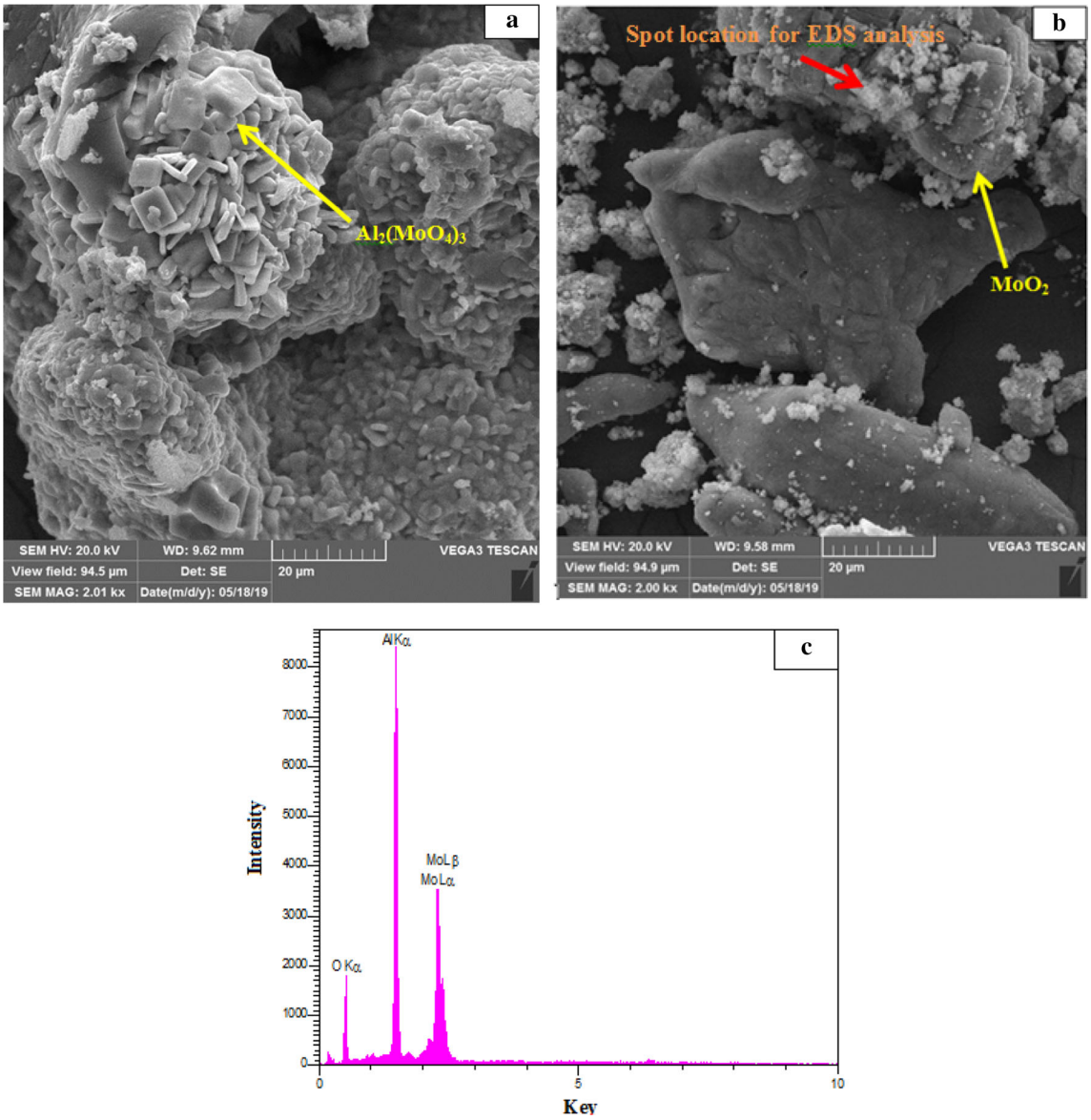

Fig. 3 The SEM micrographs of **a** un-milled $MoO_3 + Al + Al_2O_3$, **b** 24-h milled $MoO_3 + Al + Al_2O_3$ and **c** EDS analysis of 24-h milled $MoO_3 + Al + Al_2O_3$ after heat treating at 850 °C

According to Fig. 7b, it is clear that at higher temperatures, (i.e. 1100 °C), metallic Mo and $CaO{\cdot}Al_2O_3$ and a few Al_2O_3 are created as the final products. Therefore, it can be concluded that aluminothermic reduction of molybdenum trioxide in the presence of lime lead to the formation of intermediate phase, which is reduced to the final products corresponding to the third peak in Fig. 6, in the final stage of reduction process. In the presence of CaO, it chemically reacts with MoO_3 and calcium molybdate is formed at relatively low temperature according to the reaction (8) [17]:

$$MoO_3 + CaO = CaMoO_4 \quad (8)$$

The formation of $CaMoO_4$ prevents the sublimation of MoO_3. In the second step, calcium molybdate is reduced by Al to Mo and $CaO{\cdot}Al_2O_3$ according to reaction (9) [21].

$$CaMoO_4 + 2Al = Mo + CaO \cdot Al_2O_3 \quad (9)$$

The reaction (9) can be disported and be carried out in two steps. In the first step, $CaMoO_4$ is reduced by Al according to following reaction:

$$CaMoO_4 + 2Al = Mo + CaO + Al_2O_3 \quad (10)$$

This trend has been reported in the reduction of MoO_3 with carbon in the presence of CaO that can be shown as follows [17]

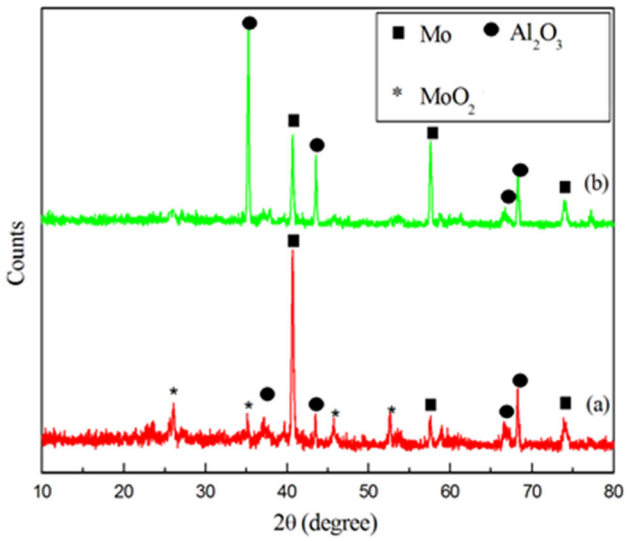

Fig. 4 The XRD patterns of **a** un-milled and **b** 24-h milled $MoO_3 + Al + Al_2O_3$ after heating up to 1100 °C

$$CaMoO_4 + 3CO_{(g)} = Mo + CaO + 3CO_2(g) \quad (11)$$

According to reaction (10) and with attention to the phase diagram of $CaO–Al_2O_3$ [21], in the second step, the produced CaO and Al_2O_3 can react with each other and forms the $CaO{\cdot}Al_2O_3$ phase that has a lower density and melting point [21]. So it can be separated easily from the molten Mo phase. In Table 1, the feasibility of reactions (8) and (9) in relation to thermodynamic calculations are shown [18]. According to Table 1, the formation of calcium molybdate by reaction (8) and finally reducing to molybdenum metal by Al is thermodynamically feasible at relatively low temperature. The second peak in the $MoO_3 + Al + CaO$ analysis is endothermic, whereas according to Table 1, formation of $CaMoO_4$ is exothermic [18]. The reason for creation of an endothermic peak in the $MoO_3 + Al + CaO$ analysis is sublimation of MoO_3, that overlaps with the peak corresponding to the formation of $CaMoO_4$. The $\Delta H°$ values for sublimation of MoO_3 in different temperatures are calculated and presented in Fig. 8. According to Table 1 and Fig. 8, the summation of $\Delta H°$ for formation of $CaMoO_4$ and sublimation of MoO_3 is positive that results in the creation of an endothermic peak in Fig. 6b. Figure 9 shows the SEM and EDS images of $MoO_3 + Al + CaO$ powder mixtures after heating up to 850 and 1100 °C.

As it can be seen in Fig. 9a, the intermediate phase in aluminothermic reduction of molybdenum trioxide in the presence of lime has a completely different morphology and shape compared to the intermediate phase created in $MoO_3 + Al + Al_2O_3$ mixture, as shown in Fig. 3a and b. The $CaMoO_4$ powder is synthesized at 800 °C (Fig. 6b) and comprises of densely agglomerated particles with the roughly spherical shapes. The EDS analysis of intermediate phase (Fig. 9b) is consistent with pure $CaMoO_4$ and with Al that is use in the next step for reducing $CaMoO_4$, according to reaction (9). Figure 9c shows that the final products in aluminothermic reduction of MoO_3 in the presence of lime are molybdenum metal and $CaO{\cdot}Al_2O_3$ in this case; coarser particles of Mo and needle shapes $CaO{\cdot}Al_2O_3$ are produced. EDS analysis of the mixture after heating up to 1100 °C (Fig. 9d) proves the presence of Ca,

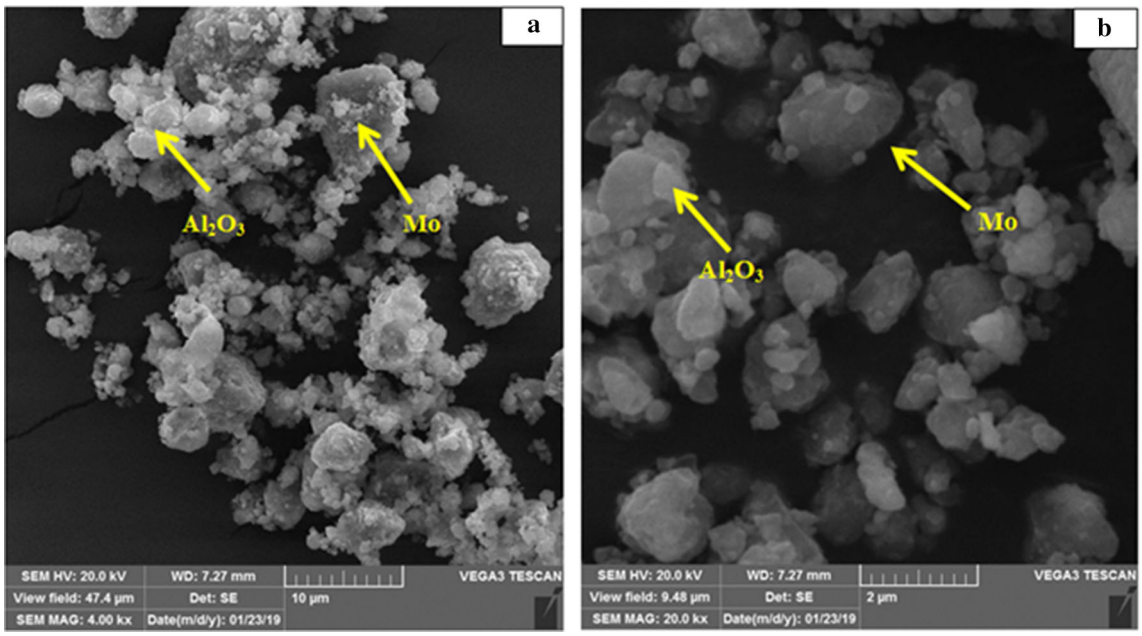

Fig. 5 The SEM micrographs of **a** un-milled $MoO_3 + Al + Al_2O_3$ and **b** 24-h milled $MoO_3 + Al + Al_2O_3$ after heating up to 1100 °C

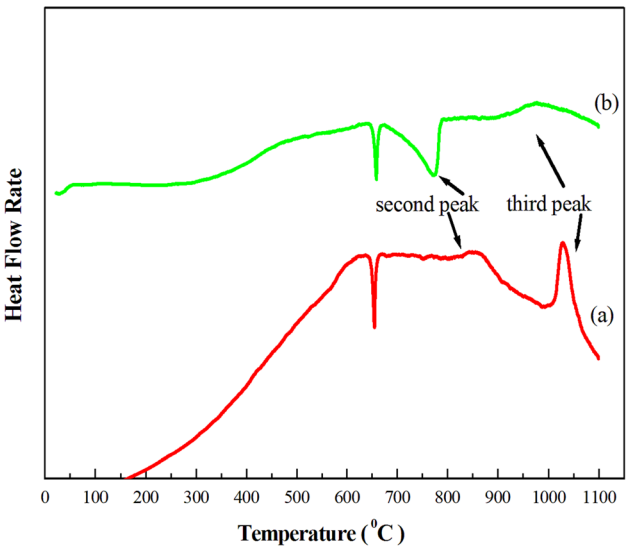

Fig. 6 DSC analysis of **a** $MoO_3 + Al + Al_2O_3$ and **b** $MoO_3 + Al + CaO$ mixtures, both including un-milled MoO_3

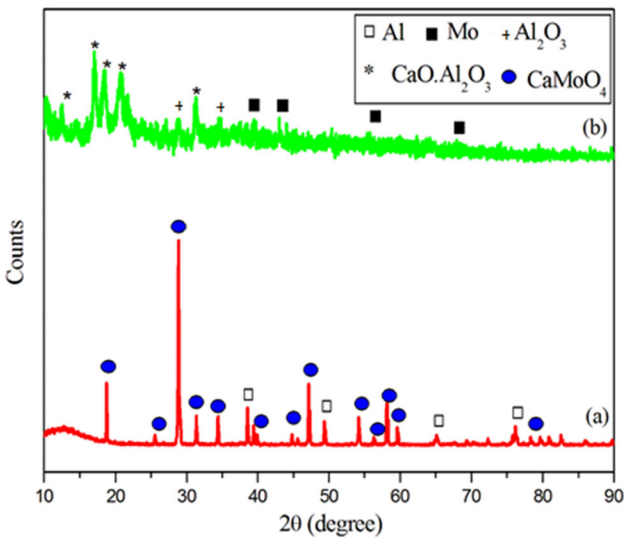

Fig. 7 The XRD patterns of the $MoO_3 + Al + CaO$ mixture after heating up to **a** 850 and **b** 1100 °C

Mo, Al and O elements that is an evidence of production of Mo and $CaO{\cdot}Al_2O_3$ as final products.

3.4 Effect of CaO Addition and Mechanical Activation on Sublimation of MoO_3 During Reduction by Al

One of the important problems in metalothermic reduction of MoO_3 is sublimation of this oxide due to its high vapor pressure. In this research, two different methods of mechanical activation and addition of CaO have been proposed for reducing the extent of MoO_3 sublimation. Figure 10 shows the TGA analysis during aluminothermic reduction of MoO_3 in three different conditions including, as received, after mechanical activation and in the presence of lime.

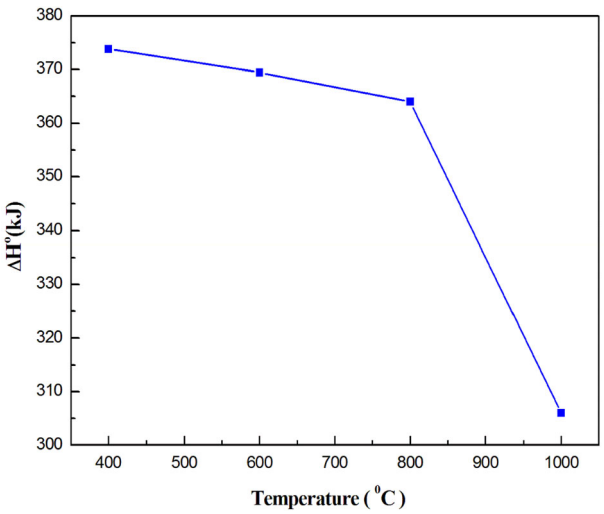

Fig. 8 $\Delta H°$ values for sublimation of MoO_3 in different temperatures [18]

Based on the literature review and the TGA analysis's results, sublimation of MoO_3 starts at temperatures above 700 °C [17]. By adding CaO to the mixture of MoO_3 and Al, according to reaction (8) and Fig. 7a, $CaMoO_4$ is formed as a thermally stable phase with low vapor pressure and therefore it can prevent sublimation of molybdenum trioxide. Mechanically activated MoO_3 also can reduce the sublimation of molybdenum trioxide by decreasing the reaction temperature for formation of MoO_2 (reaction 4). With formation of MoO_2, the sublimation of MoO_3 is prevented. To prove the production of MoO_2 at relatively low temperature, the XRD patterns for the $MoO_3 + Al + Al_2O_3$ mixture including 24-h mechanically activated MoO_3 that have been heated up to 750 °C with a heating rate of 10 °C min^{-1} is presented in Fig. 11.

According to Fig. 11 and by comparing it with Fig. 2b, it can be recognized that MoO_2 is formed at 750 °C for the mixture including 24-h mechanically activated MoO_3, thus decreasing the sublimation of MoO_3. Furthermore, as for the mechanically activated MoO_3, according to Figs. 2 and 11, the intermediate phase is MoO_2; thus higher rate of reduction to final products can be expected. In fact, for this case, formation of $Al_2(MoO_4)_3$, which is subsequently dissociated to molybdenum dioxide and aluminum oxide, is eliminated, and therefore higher rate for producing final product is expected.

3.5 Kinetic Investigation

In the present study, kinetics of the aluminothermic reduction of MoO_3 and the effects of mechanical

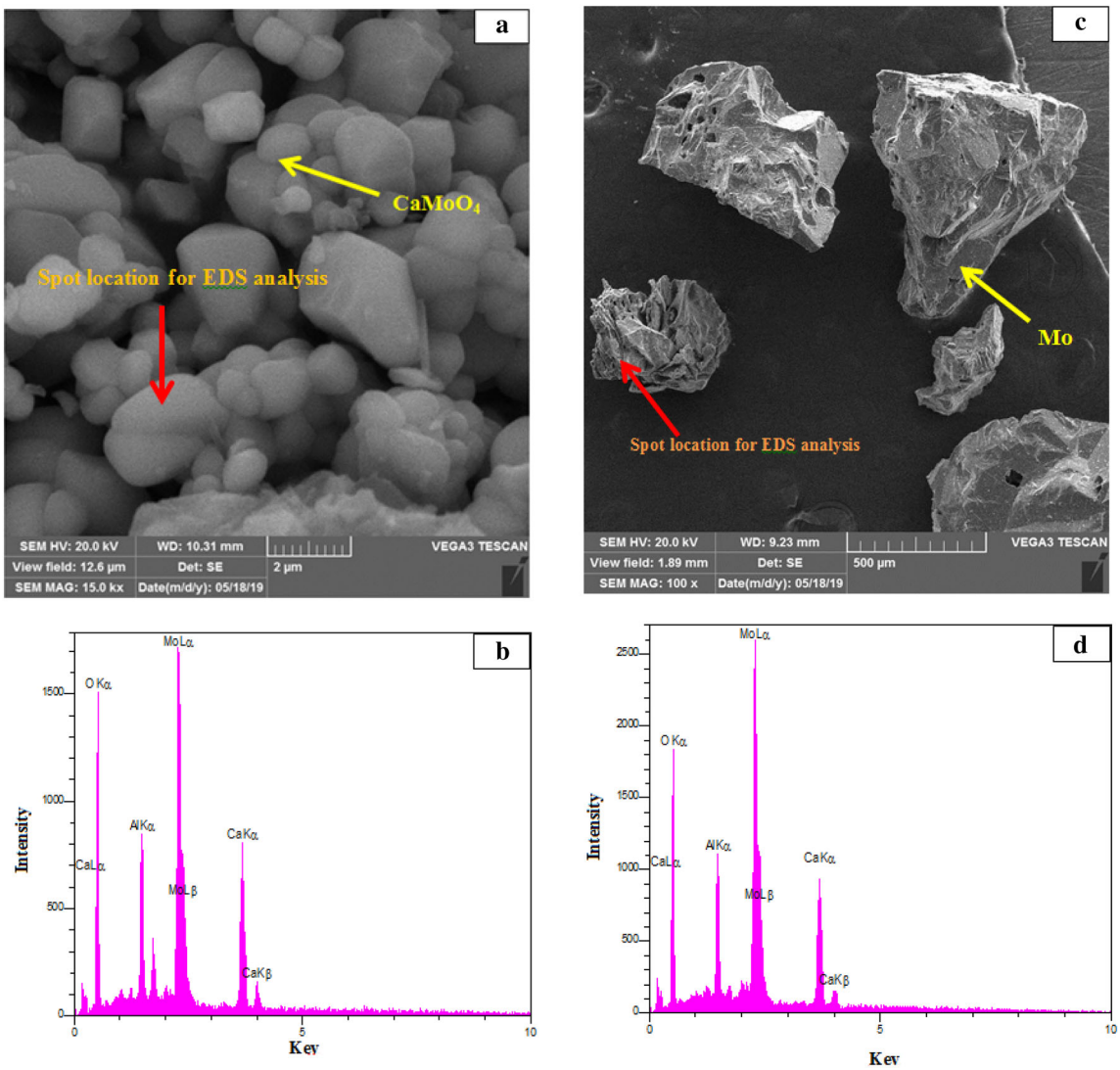

Fig. 9 SEM and EDS images of MoO_3 + Al + CaO powder mixture after heating up to 850 °C in **a** and **b** and to 1100 °C in **c** and **d**

activation and addition of CaO on it have been investigated. It is important that, the current kinetic treatment is carried out for the third peaks. So, all of current kinetic calculations have been carried out for the reduction of intermediate phases to metallic molybdenum. For this purpose, the kinetics parameters were obtained from non-isothermal rate laws using fitting methods [21, 22]. Model-fitting method involves fitting different models to the extent of reaction happened (α) versus temperature curves and simultaneously determining the activation energy (E) and pre-exponential factor (A) [23]. There are a few non-isothermal model-fitting methods, among them the Coats–Redfern method is the most popular one [24].

3.5.1 Coats–Redfern Kinetic Analysis

Coats–Redfern equation can be described by the following equation [25, 26]

$$\ln\left[g(\alpha)/T^2\right] = \ln(AR/\beta E_\alpha) - (E_\alpha/RT) \quad (12)$$

where g (α) is the integral reaction model, R, β and T are universal gas constant (8.314 J mol^{-1} K^{-1}), heating rate (K min^{-1}) and experimental temperature.

By plotting the left-hand side of Eq. (12), including the integral reaction model, versus temperature, the activation energy (E_α) and pre-exponential factor (A) can be obtained from the slope and intercept of the curve, respectively. In this method, a model, which shows the best linear fit is

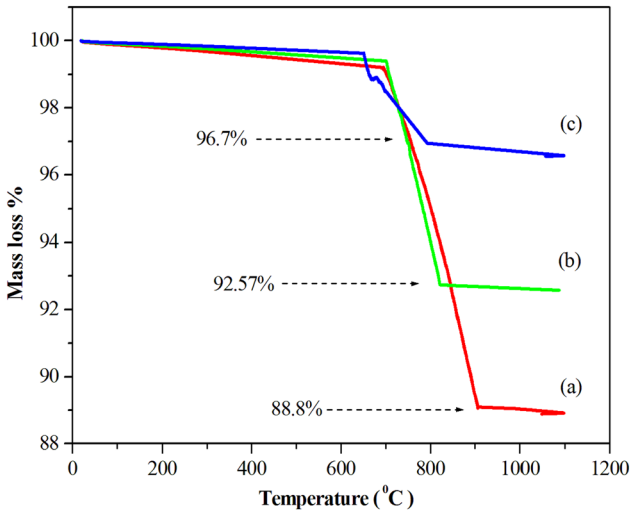

Fig. 10 TGA analysis of the $MoO_3 + Al + Al_2O_3$ mixtures including; **a** un-milled, **b** 24-h milled MoO_3 and **c** $MoO_3 + Al + CaO$ mixture

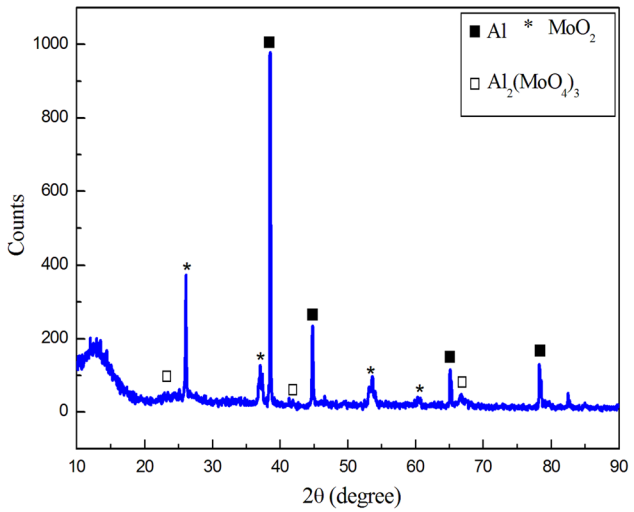

Fig. 11 XRD patterns of MoO_3 (24 h activated) + Al + Al_2O_3 mixture, heated up to 750 °C with a heating rate of 10 °C min^{-1}

selected as the kinetic model for the reactions [16]. The $g(\alpha)$ and also $f(\alpha)$ for some reaction models are listed in Table 2. The $f(\alpha)$ is the differential reaction model that has been used for calculation of the rate of reaction and temperature dependence of the process rate in the later equations.

According to Table 2, the solid-state reaction models are divided into three general categories of nucleation models, diffusion models and chemical control models (reaction order and geometrical contraction models).

Nucleation Models The first step in the process of creating a new solid phase from a supersaturated solution (either aqueous or solid) is called nucleation. A particle formed by the event of nucleation usually has a poorly ordered and often highly hydrated structure [27]. This particle is metastable with respect to ordering into a well-defined phase, which can accompany growth of the particle. This process of initiation of a new phase is defined as a first-order transition and can follow various pathways involving a host of mechanisms. One of these pathways occurs when individual nuclei coalesce into larger clusters, a process defined as aggregation, which itself can follow a series of different pathways [28].

Diffusion Models Diffusion-controlled (or diffusion-limited) reactions are reactions in which the reaction rate is equal to the rate of transport of the reactants through the reaction medium. Diffusion control is rare in the gas phase, where rates of diffusion of molecules are generally very high [29]. Diffusion control is more likely in solution where diffusion of reactants is slower due to the greater number of collisions with solvent molecules. Reactions where the activated complex forms easily and the products form rapidly are most likely to be limited by diffusion control. Heterogeneous reactions where reactants are in different phases are also candidates for diffusion control [30].

Chemical Control Models The process of chemical reaction can be considered as involving the diffusion of reactants until they encounter each other in the right stoichiometry and form an activated complex which can form the product species [31]. The observed rate of chemical reactions is, generally speaking, the rate of the slowest or rate determining step. Therefore, a surface-controlled process is characterized by the rate of molecule transport from the bulk to the interface, whereas a diffusion-controlled process is explained by the rate of molecules diffuse initially into the subsurface and then finally onto the interface [32].

The pre-exponential factors for the solid state reactions, the theoretical values are reported to be in the range of 10^6–10^{18} s^{-1} [16]. In the Coats–Redfern method, the α, as the extent of reaction, is determined using the TGA data [16], by the following equation:

$$\alpha = (W_o - W_t)/(W_o - W_f) \tag{13}$$

where W_o and W_t are the masses of the sample initially and at time t, and W_f is the sample mass at the end of reduction reaction. However, according to the reactions (1) and (2) for the aluminothermic reduction of molybdenum trioxide, there is no weight loss due to the mentioned reactions theoretically, because all reactants and products are in the solid and liquid phases. Therefore, Eq. (13) and TGA analysis cannot be used for the calculation of the extent of reaction (α) in the case of aluminothermic reduction of MoO_3. The other method for calculating (α) is by using DSC analysis data [24]. In this method, the measured rate of heat release, dQ/dt is supposed to be proportional to the

Table 2 Solid-state reaction rate models [16]

Reaction model	$f(\alpha)$	$g(\alpha)$
Nucleation models		
Power law	$4\alpha^{3/4}$	$\alpha^{1/4}$
Power law	$3\alpha^{2/3}$	$\alpha^{1/3}$
Power law	$2\alpha^{1/2}$	$\alpha^{1/2}$
Avrami–Erofeev	$4(1-\alpha)[-\ln(1-\alpha)]^{3/4}$	$[-\ln(1-\alpha)]^{1/4}$
Avrami–Erofeev	$3(1-\alpha)[-\ln(1-\alpha)]^{2/3}$	$[-\ln(1-\alpha)]^{1/3}$
Avrami–Erofeev	$2(1-\alpha)[-\ln(1-\alpha)]^{1/2}$	$[-\ln(1-\alpha)]^{1/2}$
Diffusion models		
One-dimensional diffusion	$(1/2)\alpha^{-1}$	α^2
Diffusion control (janders)	$2(1-\alpha)^{2/3}[1-(1-\alpha)^{1/3}]-1$	$[1-(1-\alpha)^{1/3}]^2$
Diffusion control (crank)	$(3/2)[(1-\alpha)^{-1/3}-1]^{-1}$	$1-(2/3)\alpha-(1-\alpha)^{2/3}$
Reaction order and geometrical contraction models		
Mample (first order)	$1-\alpha$	$-\ln(1-\alpha)$
Second order	$(1-\alpha)^2$	$(1-\alpha)^{-1}-1$
Contracting cylinder	$2(1-\alpha)^1/^2$	$1-(1-\alpha)^{1/2}$
Contracting sphere	$3(1-\alpha)^2/^3$	$1-(1-\alpha)^{1/3}$

global rate of reaction ($d\alpha/dt$), as shown in the following equation [24]:

$$dQ/dt = Q_c\, d\alpha/dt \tag{14}$$

where Q_c is the proportionality constant, which in this case is the measured heat of reaction. By integrating the DSC peaks, the values of Q_c as well as the extent of the reaction (α) can be obtained [24]. Figure 12 shows the curves of extent of the reaction (α) as a function of temperature for the MoO_3–Al–Al_2O_3 mixture including un-milled and

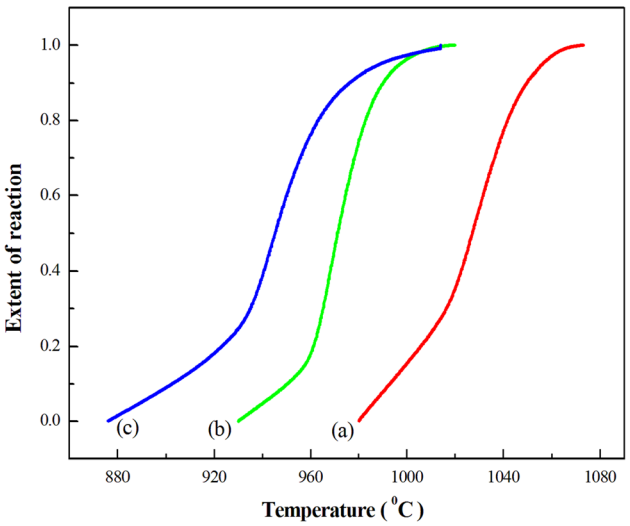

Fig. 12 Extent of reaction (α) as a function of temperature for MoO_3 + Al + Al_2O_3 mixtures including (a) un-milled, (b) 5-h milled and (c) 24-h milled MoO_3

milled MoO_3 that has been calculated by using of DSC data.

Figure 12 shows that the required temperatures for starting the aluminothermic reaction of MoO_3 decrease with increasing the activation time. According to Fig. 12, mechanically activated MoO_3 decreases the starting and ending temperature of aluminothermic reduction. These results also prove that by mechanical activation, the sublimation of MoO_3 can be expected to be decreased due to the decrease in the temperature of reactions. According to Fig. 12, the slopes of these curves are approximately in the range of 0.2–0.8, which is an indication of a constant mechanism in this range. Therefore, the value of activation energy is approximately constant in this range as has also been reported by Vyazovkin and Wight [33]. After calculating the extent of reaction (α), Arrhenius parameters are determined for all the used samples by plotting the curves of $\ln[g(\alpha)/T^2]$ versus $1/T$ in the ranges of $\alpha = 0.2$ to $\alpha = 0.8$. Figure 13 shows an example for these plots, in which the thirteenth model, introduced in Table 2, is applied for the MoO_3 + Al + Al_2O_3 mixture including un-milled MoO_3.

Arrhenius parameters (A, E_α) are determined from the plot of $\ln[g(\alpha)/T^2]$ versus T^{-1}. The set of Arrhenius parameters for the molybdenum trioxide reduction for un-milled and 24-h milled samples, based on using different models shown in Table 2, are calculated and presented in Table 3.

This calculation has also been carried out for the 5-h activated sample and MoO_3(un-milled) + Al + CaO mixture and the expected reaction mechanism, activation

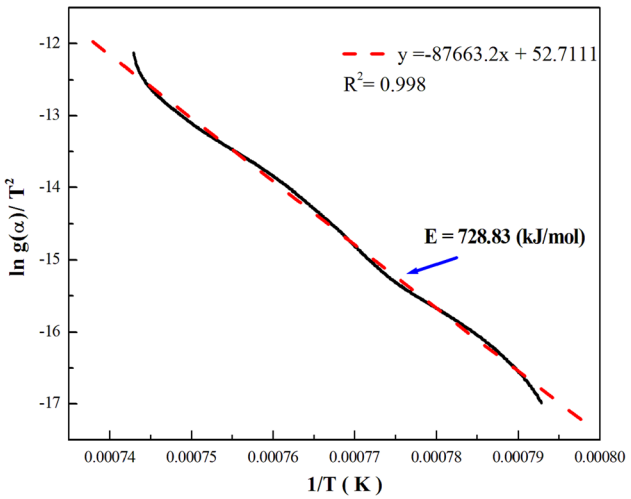

Fig. 13 The plot of ln [$g(\alpha)/T^2$] versus $1/T$ for the thirteenth model of un-milled $MoO_3 + Al + Al_2O_3$

energy and pre-exponential factor for all the used samples are determined by considering the range of the value of pre-exponential factor and highest R^2 value. The results of reaction mechanism, activation energy and pre-exponential factor for all the used samples are presented in Table 4. In the solid–solid reactions (present study), the value of activation energy is bigger than solid–gas reactions [19, 20, 24, 25]. Nevertheless for the activated MoO_3, the amount of activation energy is obtained as 336.12 and 253.22 (kJ mol^{-1}) for 5- and 24-h activated MoO_3 that is a logical result [24, 25, 27].

Regarding the information presented in Table 4, it can be suggested that the best kinetic model for fitting reaction kinetics in $MoO_3 + Al + Al_2O_3$, in which MoO_3 has been used in the form of milled and un-milled, is chemical control or Mample (first order) model, introduced in Table 2. The process of chemical reaction can be considered as involving the diffusion of reactants until they encounter each other with the right stoichiometry and form an activated complex, which can form the product species [31]. In the mixture of MoO_3 and Al including 20 wt% of Al_2O_3, chance of chemical/surface control of the reaction probably increases due to created high contact surface area between the reactants (MoO_3 and Al) due to mechanical activation process. In such a condition, it can be supposed that a surface process, which is controlled by the rate of molecule transport from the bulk to the interface, is controlling rate of the reaction [32]. But in the MoO_3 (un-milled) + Al + CaO mixture, the numbers of reactants have been increased (MoO_3, Al and CaO) and the kinetic model that can fit the reaction kinetic has been changed to diffusion control (model 8 in Table 2). Diffusion-controlled (or diffusion-limited) reactions are reactions in which the reaction rate is equal to the rate of transport of the reactants through the reaction medium [28, 29]. Diffusion control is rare in the gas phase, where rates of diffusion of molecules are generally very high [29]. Diffusion control is more likely in solution where diffusion of reactants is slower due to the greater number of collisions with solvent molecules. In the MoO_3, Al and CaO mixture, due to increase in the collisions of reactants with increase in the number of reactants, the kinetic model changes to diffusion control model [30].

As it is evidenced in Table 4, mechanical activation can reduce the activation energy that can lead to increase the rate of reaction. In the MoO_3–Al–Al_2O_3 mixture including activated and non-activated MoO_3, due to high pre-

Table 3 Arrhenius parameters for the aluminothermic reduction of un-milled and 24-h milled molybdenum trioxide, calculated based on using different models presented in Table 2

Model	Un-milled sample			24-h milled sample		
	E (kJ mol^{-1})	A (s^{-1})	R^2	E (kJ mol^{-1})	A (s^{-1})	R^2
1	114.56	42.06	0.89	64.93	0.27	0.848
2	159.77	3.52×10^3	0.898	93.54	5.34	0.866
3	250.73	20×10^6	0.906	151.13	1610	0.881
4	183.32	44.77×10^3	0.97	111.05	42.88	0.96
5	251.365	32.11×10^6	0.977	155.04	3.5×10^3	0.96
6	388.25	1.451×10^{13}	0.97	243.47	2.1×10^7	0.97
7	1067.52	7.53×10^{40}	0.901	668.35	1.87×10^{24}	0.90
8	1378.2	6.44×10^{52}	0.962	871.95	1.24×10^{32}	0.90
9	1243.5	1.7×10^{47}	0.947	773.28	7.5×10^{27}	0.93
10	418.23	1.13×10^{12}	0.999	253.22	2.43×10^{17}	0.994
11	1355.9	8.54×10^{52}	0.959	908.95	3.45×10^{35}	0.978
12	560.55	54×10^{18}	0.982	393.43	1.27×10^{13}	0.93
13	728.83	1.13×10^{18}	0.998	388.09	6.09×10^{12}	0.966

Table 4 Expected reaction mechanism, activation energy, pre-exponential factor and the equation of rate of reaction for the MoO_3 + Al + Al_2O_3 mixture including un-milled and mechanically activated MoO_3 and MoO_3 (un-milled) + Al + CaO mixture based on Coats–Redfern method

Sample	Reaction mechanism (model fitted)	E (kJ mol^{-1})	A (s^{-1})	Expected equation for the rate of reaction
MoO_3 (un-milled) + Al + Al_2O_3	Chemical control (model 10)	418.23	1.13×10^{12}	$1.13 \times 10^{12} \exp(-50304.3/T)\cdot(1-\alpha)$
MoO_3 (5 h milled) + Al + Al_2O_3	Chemical control (model 10)	336.12	8.76×10^{14}	$8.76 \times 10^{14} \exp(-40428.1/T)\cdot(1-\alpha)$
MoO_3 (24-h milled) + Al + Al_2O_3	Chemical control (model 10)	253.22	2.43×10^{17}	$2.43 \times 10^{17} \exp(-3/T).(1-\alpha)$
MoO_3 (un-milled) + Al + CaO	Diffusion control (model 8)	504.52	1.92×10^{7}	$1.92 \times 10^{7} \exp(-60683/T)\cdot(2(1-\alpha)^{2/3}[1-(1-\alpha)^{1/3}]-1)$

exponential factor and low activation energy, the rate of reaction is enough high and the mechanism of reaction is chemical control. But in the presence of CaO, according to Fig. 6b and Table 4, lower reaction temperature and lower pre-exponential factor causes the rate of reaction to decrease and the mechanism of reaction changes to diffusion control that has a slower rate in comparison with the chemical control models [16, 24]. After calculation of the Arrhenius parameters, the rate of reaction ($d\alpha/dt$) and temperature dependence of the process rate (k (T)) can be calculated. For this purpose, it is assumed that the rate of reaction is a function of only two variables, T and α in the form of two independent functions of k (T) and f (α) [24]:

$$d\alpha/dt = k(T)\cdot f(\alpha) \quad (15)$$

where f (α) is the differential reaction model that has been introduced in Table 2. The temperature dependence of the rate of process is typically parameterized through the Arrhenius equation as follows [24]:

$$K(T) = A\exp(-E_\alpha/RT) \quad (16)$$

Therefore, the rate of reaction can be calculated by combining Eqs. (15) and (16), through the following equation:

$$d\alpha/dt = A\exp(-E_\alpha/RT)\cdot f(\alpha) \quad (17)$$

The equation for the rate of reaction for the MoO_3 + Al + Al_2O_3 mixture including un-milled and milled MoO_3 and also for the MoO_3 (un-milled) + Al + CaO mixture is presented in Table 4.

According to Table 4, the values of pre-exponential factor (A) and activation energy (E) have great influence on the reaction rate. In the presence of CaO, due to lower reaction rate and lower rate constant (k (T)), the mechanism of reaction changes to diffusion control.

4 Conclusions

Based on the results and discussions presented in this study, it can be concluded that:

1 Aluminothermic reduction of molybdenum trioxide was advanced through the formation of intermediate phases of $Al_2(MoO_4)_3$ and MoO_2, where in the next step they transformed to the metallic molybdenum and aluminum oxide, as final products.
2 Using mechanically activated MoO_3 in MoO_3–Al–Al_2O_3 mixture resulted in decrease in the starting and ending temperature of aluminothermic reduction.
3 Addition of CaO to the aluminothermic reduction reaction of MoO_3 resulted in the formation of $CaMoO_4$ as the intermediate phase.
4 By 24-h milling of molybdenum trioxide or in the presence of CaO, the weight loss of MoO_3 due to sublimation was reduced from 11.2% to about 7.5% and 3.3%, respectively.
5 The model-fitting kinetic approach of DSC data showed that the kinetic model for the aluminothermic reaction of both un-milled and 24-h milled MoO_3 was chemical control model.
6 Mechanically activating MoO_3 for 24 h caused decrease in activation energy for the aluminothermic reduction from 418.23 kJ mol^{-1} for un-milled sample to 253.22 kJ mol^{-1}.
7 In the presence of CaO, activation energy of the aluminothermic reduction reaction of MoO_3 was increased and the reaction model changed to diffusion control model with E_α = 504.52 kJ mol^{-1} and $A = 1.92 \times 10^7$ s^{-1}.

References

1. Dang J, Zhang G H, Chou K C, Reddy R G, He Y, Sun Y, *Int J Refract Met Hard Mater* **41** (2013) 216.
2. Keshavarz Alamdari E, *Trans Indian Inst Met* **70** (2017) 1995.
3. Wasim S, Guodong Z H, Ghufranud D, Xiangxian M, *Trans Indian Inst Met* **72** (2019) 559.
4. Khabbaz S, Honarbakhsh-Raouf A, Ataie A, Saghafi M, *Int J Refract Met Hard Mater* **41** (2013) 402.
5. Wang D H, Sun G D, Zhang G H, *Int J Refract Met Hard Mater* **75** (2018) 70.

6. Sun G D, Zhang G H, Jiao S, Chou K C, *J Phys Chem C* **122** (2018) 1023.
7. Sun G D, Zhang G H, Ji X P, Liu J K, Zhang H, Chou K C, *Int J Refract Met Hard Mater* **80** (2019) 11.
8. Manukyan K, Aydinyan S, Aghajanyan A, Grigoryan Y, Niazyan O, Kharatyan S, *Int J Refract Met Hard Mater* **31** (2012) 28.
9. Manukyan K, Mnatsakanyan R, Kharatyan S, *Int J Refract Met Hard Mater* **28** (2010) 601.
10. Hoseinpur A, Bafghi M S, Vahdati Khaki J, *Int J Refract Met Hard Mater* **50** (2015) 191.
11. Raj R, Kumari D, Prasad R, *Trans Indian Inst Met* **72** (2019) 11.
12. Aydinyan S V, Manukyan Z, *Mater Sci Eng B* **172** (2010) 267.
13. Torabi O, Golabgir M H, Tajizadegan H, Torabi H, *Int J Refract Met Hard Mater* **47** (2014) 18.
14. Sheybani K, Paydar M H, Shariat M H, *Int J Refract Met Hard Mater* **82** (2019) 245.
15. Saghafi M, Ataie A, Heshmati-Manesh S, *Int J Refract Met Hard Mater* **29** (2011) 419.
16. Ebrahimi-Kahrizsangi R, Abbasi M H, Saidi A, *Chem Eng J* **121** (2006) 65.
17. Hung Z, Zheng L, *J Iron Steel Res Int* **21** (2013) 51.
18. Outokumpu R A, *HSC Chemistry Software*, vol. 5.1 (2002). https://www.hsc-chemistry.com/.
19. Caballero J A, Conesa J A, *J Anal Appl Pyrolysis* **73** (2005) 85.
20. Vyazovkina S, Burnhamb A K, Criadoc J M, Pere L A, Popescud C, Sbirrazzuol N, *Thermochim Acta* **520** (2011) 1.
21. Doweidar H, *J Non Cryst Solids* **471** (2017) 344.
22. Hu H P, Chen Q Y, Yin Z Y, He H Y, Huang H, *Trans Nonferr Met Soc China* **17** (2007) 205.
23. Bakhshandeh S, Setoudeh N, Askari Zamani M A, Mohassel A, *J Min Metall Sect B Metall* **54** (2018) 313.
24. Sah S, Dutta K, *Trans Indian Inst Met* **64** (2011) 583.
25. Bojan J, Srec S, Bemd F, *Trans Indian Inst Met* **67** (2014) 629.
26. Chattopadhyay C, Sarkar S, Sangal S, Mondal K, *Trans Indian Inst Met* **67** (2014) 945.
27. Kelton K F, *J Non Cryst Solids* **274** (2000) 147.
28. Spillar V, Dolejs D, *Geochim Cosmochim Acta* **131** (2014) 164.
29. Corezzi S, Fioretto D, Santucci G, Kenny J, *Polymer* **51** (2010) 5833.
30. Uche A K, Chude O, Malekian R, Maharaj B T, J *Adv Signal Process* **89** (2015) 23.
31. Nagla E, Hefny E, *J Phys Sci* **28** (2017) 129.
32. Moukhina E, *J Therm Anal Calorim* **109** (2012) 1203.
33. Vyazovkin S, Wight A, *Int Rev Phys Chem* **17** (1998) 407.

Publisher's Note Springer Nature remains neutral with regard to jurisdictional claims in published maps and institutional affiliations.